2013 IEEE/RSJ International Conference on
Intelligent Robots and Systems (IROS)
November 3-7, 2013. Tokyo, Japan

Analytical Solution to Transition Function of State Error in 1-DOF Semi-passive Dynamic Walking

Fumihiko Asano[1]

***Abstract*— In this paper, we derive the analytical solution to the transition function of the state error in 1-DOF semi-passive dynamic walking for understanding how the gait stability changes according to acceleration or deceleration. We introduce the model of an active rimless wheel (RW) as the simplest walker for analysis and linearize the equation of motion incorporating a simple control torque. Through mathematical investigations, we finally derive the analytical solution to the transition function of the state error for the stance phase as a function only of the control parameters. We discuss the accuracy of the solution obtained through comparison with the values numerically-integrated in the linearized and the nonlinear walking models.**

I. INTRODUCTION

Understanding the stability principle inherent in limit cycle walking is one of the fundamental subjects in the area of robotic legged locomotion [1][2][3][4][5]. We have proposed two major approaches to stability analysis: one is the method based on the state space representation using linearization of motion and the other is the method based on mechanical energy balance. Through investigations of passive dynamic walking of a rimless wheel (RW), we clarified that both approaches derive the same result in terms of the transition function of the state error [6]. We also mathematically showed that the stability of an underactuated bipedal gait can be explained in the same manner as a RW [7][8].

We outline the main results on 1-DOF limit cycle walking in the following. The approach based on the state space representation was firstly proposed by Coleman et al. [9] They derived the transition functions of the state error for the stance and the collision phases in a passive RW. Limit cycle walkers including RWs that achieve constraint on impact posture are the easiest models for stability analysis because we can consider only the error of the angular velocity at the collision phases and the return map is reduced to a scalar function. The scalar transition functions of the state error are very useful for understanding the physical meanings and mechanisms of the inherent stability. Following the method of Coleman et al., the author analytically derived the transition functions using linearization of motion and clarified that both the stance and the collision phases are stable [6]. Specifically, they are given as the following forms:

$$\Delta\dot{\theta}_{i+1}^{-} = \bar{Q}\Delta\dot{\theta}_i^{+}, \quad \Delta\dot{\theta}_i^{+} = \bar{R}\Delta\dot{\theta}_i^{-},$$

where the subscript "i" denotes the step number and the superscripts "$-$" and "$+$" denote immediately before and immediately after impact. In a passive RW gait, $\bar{Q} = \bar{R} = \cos\alpha$ where α is the relative angle between the two neighboring leg frames. The Poincaré return map then becomes $\bar{Q}\bar{R} = \cos^2\alpha$ and the generated gait is thus asymptotically stable.

As McGeer discussed, stable limit cycle walking exhibits various convergence properties [1]. He called the mode of $0 < \bar{Q}\bar{R} < 1$ the "speed mode" and that of $-1 < \bar{Q}\bar{R} < 0$ the "totter mode". A passive RW can exhibit only speed mode because $0 < \bar{Q}\bar{R} < 1$ always holds as mentioned. Since a RW cannot control the impact posture, some control inputs must be applied to the stance phase motion to change the convergence property. The authors then extended the method to an underactuated spoked walker with actuation [10] and to a 1-DOF active RW [11]. Through mathematical investigations, we clarified that acceleration (deceleration) always worsens (improves) the convergence speed. Our research goal is achieving the mode between the speed and the totter modes: the deadbeat mode [8][11]. This mode represented by $\bar{Q} = 0$ provides the optimal solution in terms of the convergence speed or the Gait Sensitivity Norm (GSN) [4]. As in the case of computing the eigenvalues of the Jacobian matrix for the Poincaré return map [2], however, numerical simulations must be conducted because the steady gait parameters or the discrete system responses are required for computing $\bar{Q}$ [5][6][7] or the GSN [4]. The next subject to be achieved is therefore clarifying the gait stability in terms of convergence speed without performing numerical simulations.

Based on the observations, in this paper we attempt to derive the analytical solution of $\bar{Q}$ without depending on the steady gait parameters. We mathematically show that this can be achieved by using the two major approaches we have proposed. Through numerical simulations, we compare the accuracy of the derived analytical solution with those of the linearized and the nonlinear models.

II. PASSIVE DYNAMIC WALKING OF RIMLESS WHEEL

A. Stability of Passive-dynamic Gait

This section explains the stability principle of a passive eight-legged RW that walks on the slope of ϕ [rad] as shown in Fig. 1 ($\alpha = \pi/4$ [rad]) from the viewpoint of the mechanical energy balance approach [6].

We assume that the parameters with the subscript "eq" are those of the equilibrium point at the collision phase, and that the parameters with the superscript "$*$" are those of the stationary orbit.

[1]F. Asano is with the School of Information Science, Japan Advanced Institute of Science and Technology, 1-1 Asahidai, Nomi, Ishikawa 923-1292, Japan fasano@jaist.ac.jp

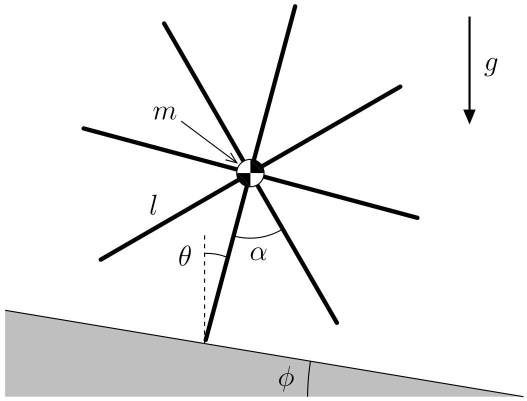

Fig. 1. Passive rimless wheel model

Let K_i^- [J] be the kinetic energy immediately before the (i)th impact. This is given by

$$K_i^- = \frac{1}{2} m l^2 \left(\dot{\theta}_i^- \right)^2 . \tag{1}$$

This can be applied for both the nonlinear and the linearized models. The following recurrence formula then holds.

$$K_{i+1}^- = \varepsilon K_i^- + \Delta E \tag{2}$$

Where $\varepsilon = \cos^2 \alpha$ [-] is the energy-loss coefficient and ΔE [J] is the restored mechanical energy supplied by gravity. Both ε and ΔE are positive constants. The potential energies immediately before and immediately after impact are given by

$$P^{\pm} = mgl \cos \left(\phi \mp \frac{\alpha}{2} \right) . \tag{3}$$

ΔE then becomes

$$\Delta E = P^+ - P^- = 2mgl \sin \frac{\alpha}{2} \sin \phi . \tag{4}$$

In the linearized model, the corresponding potential energy is defined as

$$P = mgl \left(1 - \frac{\theta^2}{2} \right) . \tag{5}$$

This derives the gravity term of the linearized RW dynamics according to the Lagrangian method [6]. The potential energies immediately before and immediately after impact then becomes

$$P^{\pm} = mgl \left(1 - \frac{1}{2} \left(\phi \mp \frac{\alpha}{2} \right)^2 \right) = P_{\max} - \frac{mgl}{2} \left(\phi \mp \frac{\alpha}{2} \right)^2 , \tag{6}$$

where $P_{\max} := mgl$ [J] is the maximum potential energy the RW can achieve. In the same way, ΔE corresponding to the linearized model becomes

$$\Delta E = P^+ - P^- = mgl\alpha\phi . \tag{7}$$

The limit value of K_i^- in the linearized model then becomes

$$K_{\text{eq}}^- := \lim_{i \to \infty} K_i^- = \frac{\Delta E}{1 - \varepsilon} = \frac{mgl\alpha\phi}{\sin^2 \alpha} . \tag{8}$$

This shows that the generated passive gait always becomes 1-period and asymptotically stable.

B. Condition for Overcoming Potential Barrier

A potential barrier exists during the stance phase in the case that the following inequality holds.

$$\theta_{\text{eq}}^+ = -\frac{\alpha}{2} + \phi < 0 \tag{9}$$

To overcome the potential barrier, the following inequality must be satisfied.

$$\begin{aligned} E_{\text{eq}}^{\pm} - P_{\max} &= K_{\text{eq}}^- + P^- - P_{\max} \\ &= \frac{mgl\alpha\phi}{\sin^2 \alpha} - \frac{mgl}{2} \left(\phi + \frac{\alpha}{2} \right)^2 > 0 \end{aligned} \tag{10}$$

This can be solved as

$$\frac{\alpha}{2} \tan^2 \frac{\alpha}{2} < \phi < \frac{\alpha}{2} \cot^2 \frac{\alpha}{2} . \tag{11}$$

By summarizing Eqs. (9) and (11), the condition necessary for overcoming the potential barrier is finally specified as

$$\frac{\alpha}{2} \tan^2 \frac{\alpha}{2} < \phi < \frac{\alpha}{2} . \tag{12}$$

The upper bound is conservative because the vertical (normal) ground reaction force becomes negative before reaching $\phi = \alpha/2$.

III. ACTIVE COMBINED RIMLESS WHEEL AND SEMI-PASSIVE DYNAMIC WALKING

A. Equations of Motion and Its Linearization

In this section, we consider the model of a planar active combined RW (CRW) shown in Fig. 2 as a realistic 1-DOF active RW model [11]. This is composed of two identical eight-legged RWs and a body frame, and can exert a joint torque, u [N·m], between the rear stance-leg and the body frame. We assume the following statements.

- The fore and rear stance legs always contact with the ground without sliding.
- The inertia moments about the CoMs of all the frames can be neglected.
- The fore and rear RWs perfectly synchronize or rotate maintaining the relation $\theta_1 \equiv \theta_2$.

This model configurates a four-bar linkage, and exerting the joint torque, u, is thus equivalent to exerting that at the contact point with the ground (ankle-joint torque). The

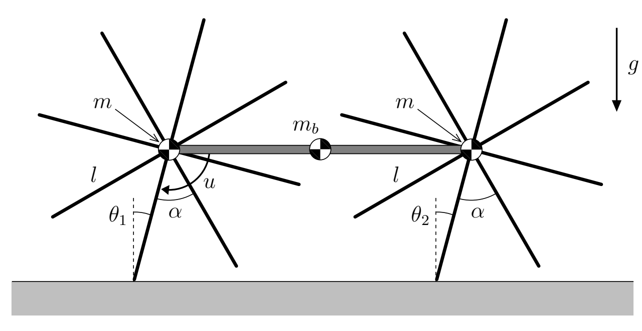

Fig. 2. Model of planar active combined rimless wheel

dynamics of the rear RW then becomes identical to that of an active RW with an ankle-joint torque, that is,

$$\ddot{\theta} = \omega^2 \sin\theta + \frac{u}{Ml^2}, \tag{13}$$

where $M := m_b + 2m$ [kg] is the total mass of the CRW, $\theta(= \theta_1 = \theta_2)$ is the stance-leg angle, and $\omega := \sqrt{g/l}$ [rad/s]. By linearizing this around $\theta = \dot{\theta} = 0$, the state-space realization of the RW dynamics becomes

$$\frac{\mathrm{d}}{\mathrm{d}t}\begin{bmatrix}\theta\\ \dot{\theta}\end{bmatrix} = \begin{bmatrix}0 & 1\\ \omega^2 & 0\end{bmatrix}\begin{bmatrix}\theta\\ \dot{\theta}\end{bmatrix} + \begin{bmatrix}0\\ 1/Ml^2\end{bmatrix}u. \tag{14}$$

In the following, we denote Eq. (14) as $\dot{\boldsymbol{x}} = \boldsymbol{A}\boldsymbol{x} + \boldsymbol{B}u$.

B. Collision Equations

We assume that the rear leg frame at impact (the previous stance leg) begins to leave the ground immediately after landing of the fore leg frame (the next stance leg) according to the law of inelastic collision. The transition equation for the angular velocity then becomes the same as that of a single RW, that is,

$$\dot{\theta}_i^+ = \cos\alpha \cdot \dot{\theta}_i^-.$$

In a steady gait, this should be

$$\dot{\theta}_{\mathrm{eq}}^+ = \cos\alpha \cdot \dot{\theta}_{\mathrm{eq}}^-.$$

Therefore the relation between the state errors immediately before and immediately after impact becomes

$$\Delta\dot{\theta}_i^+ = \cos\alpha \cdot \Delta\dot{\theta}_i^-,$$

where $\Delta\dot{\theta}_i^\pm := \dot{\theta}_i^\pm - \dot{\theta}_{\mathrm{eq}}^\pm$.

The angular positions immediately before and immediately after impact are always

$$\theta_i^\pm = \theta_{\mathrm{eq}}^\pm = \phi \mp \frac{\alpha}{2},$$

and their errors are thus always zeros. The collision phase is therefore stable.

C. Transition Function of State Error for Stance Phase

The details of the derivation originally studied by Coleman et al. [9] have already been described in our previous papers [6][8], so we outline it here.

The state vector immediately before the $(i+1)$th impact, $\boldsymbol{x}_{i+1}^-$, is written by that immediately after the (i)th impact, $\boldsymbol{x}_i^+$, as

$$\boldsymbol{x}_{i+1}^- = \mathrm{e}^{\boldsymbol{A}T_i}\boldsymbol{x}_i^+ + \int_{0^+}^{T_i^-} \mathrm{e}^{\boldsymbol{A}(T_i - s)}\boldsymbol{B}u(s)\ \mathrm{d}s. \tag{15}$$

Here, T_i [s] is the step period of the (i)th step. s is the time parameter that is reset to zero at every impact and $u(s)$ is the control torque determined as follows.

$$u(s) = \begin{cases} u_0 & (0 \le s < T_{\mathrm{set}})\\ 0 & (s \ge T_{\mathrm{set}})\end{cases} \tag{16}$$

We call T_{set} the settling time and assume that the step period is longer than T_{set}, that is, the inequality $T_i > T_{\mathrm{set}}$ must hold. The feed-forward control of Eq. (16) must be completed before the next impact (settling-time condition).

Define a constant vector $\boldsymbol{\eta} \in \mathbb{R}^2$ as

$$\begin{aligned}\boldsymbol{\eta} &:= \int_{0^+}^{T_{\mathrm{set}}} \mathrm{e}^{-\boldsymbol{A}s}\boldsymbol{B}u_0\ \mathrm{d}s\\ &= \frac{u_0}{M\omega^2 l^2}\begin{bmatrix}1 - \cosh(\omega T_{\mathrm{set}})\\ \omega\sinh(\omega T_{\mathrm{set}})\end{bmatrix} =: \begin{bmatrix}\eta_1\\ \eta_2\end{bmatrix}.\end{aligned} \tag{17}$$

Eq. (15) is then arranged as

$$\boldsymbol{x}_{i+1}^- = \mathrm{e}^{\boldsymbol{A}T_i}\left(\boldsymbol{x}_i^+ + \boldsymbol{\eta}\right). \tag{18}$$

We also define $\boldsymbol{x}_i'$ and $\boldsymbol{x}_{\mathrm{eq}}'$ here as

$$\boldsymbol{x}_i' := \boldsymbol{x}_i^+ + \boldsymbol{\eta} = \begin{bmatrix}\theta_i^+ + \eta_1\\ \dot{\theta}_i^+ + \eta_2\end{bmatrix} =: \begin{bmatrix}\theta_i'\\ \dot{\theta}_i'\end{bmatrix}, \tag{19}$$

$$\boldsymbol{x}_{\mathrm{eq}}' := \boldsymbol{x}_{\mathrm{eq}}^+ + \boldsymbol{\eta} = \begin{bmatrix}\theta_{\mathrm{eq}}^+ + \eta_1\\ \dot{\theta}_{\mathrm{eq}}^+ + \eta_2\end{bmatrix} =: \begin{bmatrix}\theta_{\mathrm{eq}}'\\ \dot{\theta}_{\mathrm{eq}}'\end{bmatrix}. \tag{20}$$

Eq. (18) is then rewritten as

$$\boldsymbol{x}_{i+1}^- = \mathrm{e}^{\boldsymbol{A}T_i}\boldsymbol{x}_i'. \tag{21}$$

In a steady gait, Eq. (21) should be

$$\boldsymbol{x}_{\mathrm{eq}}^- = \mathrm{e}^{\boldsymbol{A}T^*}\boldsymbol{x}_{\mathrm{eq}}'. \tag{22}$$

Eqs. (21) and (22) are equivalent to the linearized dynamics of a passive RW whose initial conditions are $\boldsymbol{x}_i'$ or $\boldsymbol{x}_{\mathrm{eq}}'$. Eq. (21) is expanded to

$$\begin{aligned}\boldsymbol{x}_{i+1}^- &= \mathrm{e}^{\boldsymbol{A}(T^* + \Delta T_i)}\left(\boldsymbol{x}_{\mathrm{eq}}' + \Delta\boldsymbol{x}_i^+\right)\\ &= \mathrm{e}^{\boldsymbol{A}\Delta T_i}\mathrm{e}^{\boldsymbol{A}T^*}\left(\boldsymbol{x}_{\mathrm{eq}}' + \Delta\boldsymbol{x}_i^+\right)\\ &\approx \left(\boldsymbol{I}_2 + \boldsymbol{A}\Delta T_i\right)\mathrm{e}^{\boldsymbol{A}T^*}\left(\boldsymbol{x}_{\mathrm{eq}}' + \Delta\boldsymbol{x}_i^+\right) &(23)\\ &= \mathrm{e}^{\boldsymbol{A}T^*}\left(\boldsymbol{x}_{\mathrm{eq}}' + \Delta\boldsymbol{x}_i^+\right)\\ &\quad + \boldsymbol{A}\mathrm{e}^{\boldsymbol{A}T^*}\left(\boldsymbol{x}_{\mathrm{eq}}' + \Delta\boldsymbol{x}_i^+\right)\Delta T_i. &(24)\end{aligned}$$

Here, the errors were defined as $\Delta\boldsymbol{x}_i^\pm := \boldsymbol{x}_i^\pm - \boldsymbol{x}_{\mathrm{eq}}^\pm$ and $\Delta T_i := T_i - T^*$. In addition, we used the following approximation:

$$\mathrm{e}^{\boldsymbol{A}\Delta T_i} \approx \boldsymbol{I}_2 + \boldsymbol{A}\Delta T_i. \tag{25}$$

By considering Eq. (22), Eq. (24) is further arranged as

$$\boldsymbol{x}_{i+1}^- \approx \boldsymbol{x}_{\mathrm{eq}}^- + \boldsymbol{A}\boldsymbol{x}_{\mathrm{eq}}^-\Delta T_i + \mathrm{e}^{\boldsymbol{A}T^*}\Delta\boldsymbol{x}_i^+. \tag{26}$$

Here, we neglected the error term higher than second order, that is,

$$\Delta\boldsymbol{x}_i^+\Delta T_i \approx \boldsymbol{0}_{2\times 1}. \tag{27}$$

Define $\boldsymbol{p} := \begin{bmatrix}1 & 0\end{bmatrix}$ and multiplying $\boldsymbol{x}$ by $\boldsymbol{p}$ leads to $\boldsymbol{p}\boldsymbol{x} = \theta$. Therefore, the following relation

$$\boldsymbol{p}\boldsymbol{x}_i^- = \boldsymbol{p}\boldsymbol{x}_{\mathrm{eq}}^- = \theta_{\mathrm{eq}}^- = \phi - \frac{\alpha}{2}$$

holds immediately before impact. By multiplying both sides of Eq. (26) by $\boldsymbol{p}$, we get

$$0 = \boldsymbol{p}\boldsymbol{A}\boldsymbol{x}_{\mathrm{eq}}^-\Delta T_i + \boldsymbol{p}\mathrm{e}^{\boldsymbol{A}T^*}\Delta\boldsymbol{x}_i^+. \tag{28}$$

ΔT_i is then solved as

$$\Delta T_i = -\frac{\boldsymbol{p}\mathrm{e}^{\boldsymbol{A}T^*}\Delta\boldsymbol{x}_i^+}{\boldsymbol{p}\boldsymbol{A}\boldsymbol{x}_{\mathrm{eq}}^-}.$$

By substituting this into Eq. (26) and considering the relation of $\Delta\boldsymbol{x}_{i+1}^- = \boldsymbol{x}_{i+1}^- - \boldsymbol{x}_{\text{eq}}^-$, the transition matrix of the state error is finally derived as

$$\Delta\boldsymbol{x}_{i+1}^- = \boldsymbol{Q}\Delta\boldsymbol{x}_i^+, \quad \boldsymbol{Q} := \left(\boldsymbol{I}_2 - \frac{\boldsymbol{A}\boldsymbol{x}_{\text{eq}}^-\boldsymbol{p}}{\boldsymbol{p}\boldsymbol{A}\boldsymbol{x}_{\text{eq}}^-}\right)\mathrm{e}^{\boldsymbol{A}T^*}. \quad (29)$$

Considering the relation $\dot{\boldsymbol{x}}_{\text{eq}}^- = \boldsymbol{A}\boldsymbol{x}_{\text{eq}}^-$, $\boldsymbol{Q}$ can be also formed as

$$\boldsymbol{Q} := \left(\boldsymbol{I}_2 - \frac{\dot{\boldsymbol{x}}_{\text{eq}}^-\boldsymbol{p}}{\boldsymbol{p}\dot{\boldsymbol{x}}_{\text{eq}}^-}\right)\mathrm{e}^{\boldsymbol{A}T^*}. \quad (30)$$

By considering the relation:

$$\Delta\boldsymbol{x}_i^\pm = \boldsymbol{v}\Delta\dot{\theta}_i^\pm, \quad \boldsymbol{v} := \begin{bmatrix} 0 \\ 1 \end{bmatrix},$$

$\boldsymbol{Q}$ can be reduced to the following scalar function:

$$\bar{Q} = \boldsymbol{v}^{\mathrm{T}}\boldsymbol{Q}\boldsymbol{v} = \cosh(\omega T^*) - \frac{\theta_{\text{eq}}^-\omega}{\dot{\theta}_{\text{eq}}^-}\sinh(\omega T^*). \quad (31)$$

In the following, we arrange $\bar{Q}$ into the form without depending on the steady step period, T^*. We outline the proof. Eq. (22) can be deformed to $\boldsymbol{x}_{\text{eq}}' = \mathrm{e}^{-\boldsymbol{A}T^*}\boldsymbol{x}_{\text{eq}}^-$ which is detailed as

$$\begin{bmatrix} \theta_{\text{eq}}' \\ \dot{\theta}_{\text{eq}}' \end{bmatrix} = \begin{bmatrix} \cosh(\omega T^*) & -\omega^{-1}\sinh(\omega T^*) \\ -\omega\sinh(\omega T^*) & \cosh(\omega T^*) \end{bmatrix}\begin{bmatrix} \theta_{\text{eq}}^- \\ \dot{\theta}_{\text{eq}}^- \end{bmatrix}.$$

By extracting the second row, we get

$$\dot{\theta}_{\text{eq}}' = \dot{\theta}_{\text{eq}}^-\cosh(\omega T^*) - \theta_{\text{eq}}^-\omega\sinh(\omega T^*). \quad (32)$$

Following Eqs. (31) and (32), we get

$$\frac{\dot{\theta}_{\text{eq}}'}{\dot{\theta}_{\text{eq}}^-} = \cosh(\omega T^*) - \frac{\theta_{\text{eq}}^-\omega}{\dot{\theta}_{\text{eq}}^-}\sinh(\omega T^*) = \bar{Q}. \quad (33)$$

$\bar{Q}$ can be written as the ratio of the steady angular velocities. Considering the relation of Eq. (20), Eq. (33) can be arranged as follows.

$$\bar{Q} = \frac{\dot{\theta}_{\text{eq}}^+ + \eta_2}{\dot{\theta}_{\text{eq}}^-} = \cos\alpha + \frac{u_0\sinh(\omega T_{\text{set}})}{M\omega l^2\dot{\theta}_{\text{eq}}^-} \quad (34)$$

From Eq. (34), we can understand that $\bar{Q}$ becomes $\cos\alpha$, the value in passive dynamic walking, by choosing u_0 or T_{set} as zero, and that acceleration always worsens the convergence speed whereas deceleration always improves it.

IV. ANALYTICAL SOLUTION OF $\bar{Q}$

Let t [s] be the time parameter and assume that a collision for stance-leg exchange occurs at $t = 0$ [s]. The steady state vector at t, $\boldsymbol{x}^*(t)$, then becomes

$$\boldsymbol{x}^*(t) = \mathrm{e}^{\boldsymbol{A}t}\boldsymbol{x}_{\text{eq}}^+ + \int_{0+}^{t}\mathrm{e}^{\boldsymbol{A}(t-s)}\boldsymbol{B}u_0\,\mathrm{d}s. \quad (35)$$

By extracting the first row from $\boldsymbol{x}^*(t)$ and replacing t with T_{set}, we get

$$\theta^*(T_{\text{set}}) = \frac{1}{Mgl}\Big(\Big(u_0 + Mgl\Big(\phi - \frac{\alpha}{2}\Big)\Big)\cosh(\omega T_{\text{set}}) - u_0 + \dot{\theta}_{\text{eq}}^- M\omega l^2 u_0\cos\alpha\sinh(\omega T_{\text{set}})\Big). \quad (36)$$

Next, let us revisit the recurrence formula of Eq. (2). In the case of semi-passive dynamic walking, the kinetic energy immediately before impact satisfies the following recurrence formula:

$$K_{i+1}^- = \varepsilon K_i^- + \Delta E_i, \quad (37)$$

where ε is the same as in Eq. (2) and ΔE_i [J] is the restored mechanical energy in the (i)th step. If the generated gait is asymptotically stable, Eq. (37) should converge to

$$K_{\text{eq}}^- = \varepsilon K_{\text{eq}}^- + \Delta E^*, \quad (38)$$

where ΔE^* [J] is the steady restored mechanical energy supplied by the actuation and gravity. This can be derived as

$$\begin{aligned}\Delta E^* &= \int_{0+}^{T_{\text{set}}}\dot{\theta}^* u_0\,\mathrm{d}s + Mgl\alpha\phi \\ &= \left(\theta^*(T_{\text{set}}) - \theta_{\text{eq}}^+\right)u_0 + Mgl\alpha\phi. \quad (39)\end{aligned}$$

The steady kinetic energy immediately before impact also becomes

$$K_{\text{eq}}^- = \frac{1}{2}Ml^2\left(\dot{\theta}_{\text{eq}}^-\right)^2 = \frac{\Delta E^*}{1-\varepsilon}. \quad (40)$$

Following Eqs. (36), (39) and (40) and considering $\dot{\theta}_{\text{eq}}^- > 0$, we can solve $\dot{\theta}_{\text{eq}}^-$ as

$$\dot{\theta}_{\text{eq}}^- = \frac{u_0\cos\alpha\sinh(\omega T_{\text{set}}) + \sqrt{F(u_0, T_{\text{set}})}}{M\omega l^2\sin^2\alpha}, \quad (41)$$

where F is a function of u_0 and T_{set} and can be arranged as a quadratic function of u_0 as follows.

$$F(u_0, T_{\text{set}}) = C_2u_0^2 + C_1u_0 + C_0 \quad (42)$$

The coefficients in Eq. (42) are detailed as

$$\begin{aligned}C_2 &= 2\left(\cosh(\omega T_{\text{set}}) - 1\right)\sin^2\alpha + \cos^2\alpha\sinh^2(\omega T_{\text{set}}), \\ C_1 &= -2Mgl(\alpha - 2\phi)\sin^2\alpha\sinh^2\left(\frac{\omega T_{\text{set}}}{2}\right), \\ C_0 &= 2M^2g^2l^2\alpha\phi\sin^2\alpha.\end{aligned}$$

Eq. (42) is a parabola convex downward because C_2 is positive. Fig. 3 plots the value of F with respect to u_0 and

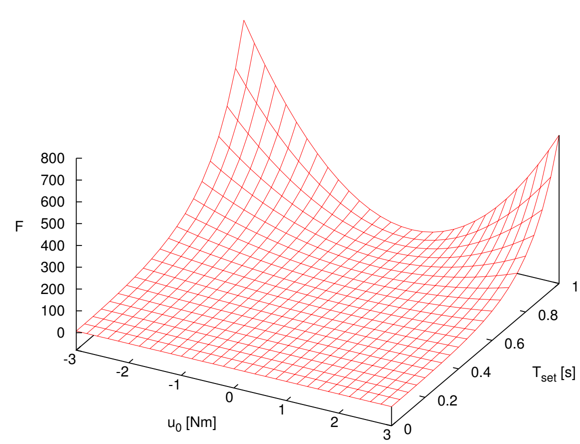

Fig. 3. F with respect to u_0 and T_{set} where $M = 1.0$ [kg], $l = 1.0$ [m] and $\phi = 0.1$ [rad]

$T_{\rm set}$ where the system parameters are chosen as $M = 1.0$ [kg], $l = 1.0$ [m] and $\phi = 0.1$ [rad]. We can confirm that F forms a parabola convex downward as a function of u_0. The minimum value of F becomes

$$F_{\rm min}(T_{\rm set}) = \frac{M^2 g^2 l^2 \sin^2\alpha G(T_{\rm set})}{8\left(2+\cos^2\alpha\left(\cosh(\omega T_{\rm set})-1\right)\right)}, \quad (43)$$

where

$$\begin{aligned} G(T_{\rm set}) =& \ \alpha^2 + 20\alpha\phi + 4\phi^2 \\ & -\left(\alpha^2 - 12\alpha\phi + 4\phi^2\right)\cosh(\omega T_{\rm set}) \\ & +2(\alpha+2\phi)^2\cos(2\alpha)\sinh^2\left(\frac{\omega T_{\rm set}}{2}\right). \quad (44) \end{aligned}$$

Since the denominator of $F_{\rm min}$ is always positive, the sign of $F_{\rm min}$ is equal to that of $G(T_{\rm set})$. The partial derivative of $G(T_{\rm set})$ with respect to $T_{\rm set}$ becomes

$$\begin{aligned} \frac{\partial G(T_{\rm set})}{\partial T_{\rm set}} =& \left(-\alpha^2 + 12\alpha\phi - \phi^2 + (\alpha+2\phi)^2\cos(2\alpha)\right) \\ & \times\omega\sinh(\omega T_{\rm set}). \quad (45) \end{aligned}$$

We then obtain the following relation.

$$\frac{\partial G(T_{\rm set})}{\partial T_{\rm set}} > 0 \iff \frac{\alpha}{2}\tan^2\frac{\alpha}{2} < \phi < \frac{\alpha}{2}\cot^2\frac{\alpha}{2} \quad (46)$$

This is included in Eq. (12). Therefore we can conclude that $G(T_{\rm set})$ monotonically increases from $G(0) = 32\alpha\phi > 0$ with the increase of $T_{\rm set}$ if the condition of Eq. (12) is satisfied or the walker can exhibit passive dynamic walking. Note that, however, this condition is sufficient and conservative. The positivity of $G(T_{\rm set})$ is not always necessary for $F_{\rm min}(T_{\rm set}) \geq 0$.

By substituting $\dot{\theta}_{\rm eq}^-$ of Eq. (41) into Eq. (34), $\bar{Q}$ can be derived as a function of u_0 and $T_{\rm set}$ as

$$\bar{Q}\left(u_0, T_{\rm set}\right) = \frac{u_0\sinh\left(\omega T_{\rm set}\right) + \cos\alpha\sqrt{F(u_0, T_{\rm set})}}{u_0\cos\alpha\sinh\left(\omega T_{\rm set}\right) + \sqrt{F(u_0, T_{\rm set})}}. \quad (47)$$

Although it is obvious, Eq. (47) has the following limit values in the case without actuation, i.e. passive dynamic walking.

$$\bar{Q}\left(0, T_{\rm set}\right) = \cos\alpha, \quad \bar{Q}\left(u_0, 0\right) = \cos\alpha$$

Let us define

$$\nabla\bar{Q}_x\left(u_0, T_{\rm set}\right) := \frac{\partial\bar{Q}\left(u_0, T_{\rm set}\right)}{\partial x}.$$

The partial derivative of $\bar{Q}$ with respect to $T_{\rm set}$ where $T_{\rm set} = 0$ then becomes

$$\nabla\bar{Q}_{T_{\rm set}}\left(u_0, 0\right) = \frac{u_0\omega\sin\alpha}{\sqrt{2\alpha\phi}Mgl}. \quad (48)$$

The sign of Eq. (48) is the same as that of u_0. Therefore, as suggested by Eq. (34), the convergence speed monotonically worsens with the increase of $T_{\rm set}$ if u_0 is positive.

On the other hand, the partial derivative of $\bar{Q}$ with respect to u_0 where $u_0 = 0$ becomes

$$\nabla\bar{Q}_{u_0}\left(0, T_{\rm set}\right) = \frac{\sin\alpha\sinh\left(\omega T_{\rm set}\right)}{\sqrt{2\alpha\phi}Mgl}. \quad (49)$$

This is always positive and $\bar{Q}$ therefore monotonically increases with the increase of u_0.

V. NUMERICAL ANALYSIS

This section evaluates the accuracy of the analytical solution of Eq. (47) by comparing with the values numerically-integrated in the linearized and the nonlinear walking models.

A. Effect of $T_{\rm set}$

Let us define the real transition function of the state error for the stance phase of the (i)th step, $\bar{Q}_i$, as

$$\bar{Q}_i := \frac{\Delta\dot{\theta}_{i+1}^-}{\Delta\dot{\theta}_i^+}. \quad (50)$$

Here, we should remember that the analytical solution of $\bar{Q}$ was derived by using two linear approximations of Eqs. (25) and (26). It is then expected that $\bar{Q}_i$ would return different values from the analytical solution.

Fig. 4 shows the evolution of $\bar{Q}_i$ with respect to the step number where $T_{\rm set} = 0.1$ [s], $u_0 = 1.0$ [s] and $\phi = 0.1$ [rad] in the linearized model and its magnified view. We can see that the value seems mostly unchanged for the initial steps but it begins to violate later. This is because the denominator of Eq. (50) converges to zero as well as the numerator, that is, Eq. (50) finally becomes an indeterminate form. Therefore we can take the values only for the first several steps for evaluation. As shown in the magnified view in Fig. 4, however, there is considerable changes in $\bar{Q}$ for the initial steps due to the error terms higher than second order neglected. We then numerically compute the value of $\bar{Q}$ for the linearized and the nonlinear models as the mean value of $\bar{Q}$ for the first five steps:

$$\bar{Q} := \frac{1}{5}\sum_{i=0}^{4}\bar{Q}_i. \quad (51)$$

Fig. 5 plots $\bar{Q}$ of Eq. (51) in the linear and the nonlinear models and the analytical solution of $\bar{Q}$ of Eq. (47) with respect to $T_{\rm set}$ where $M = 1.0$ [kg], $l = 1.0$ [m], $u_0 = 1.0$ [N·m] and $\phi = 0.1$ [rad]. The initial angular velocity is chosen as $\dot{\theta}_0^+ = \dot{\theta}_{\rm eq}^+ + 0.2$ [rad/s]. As the mathematical

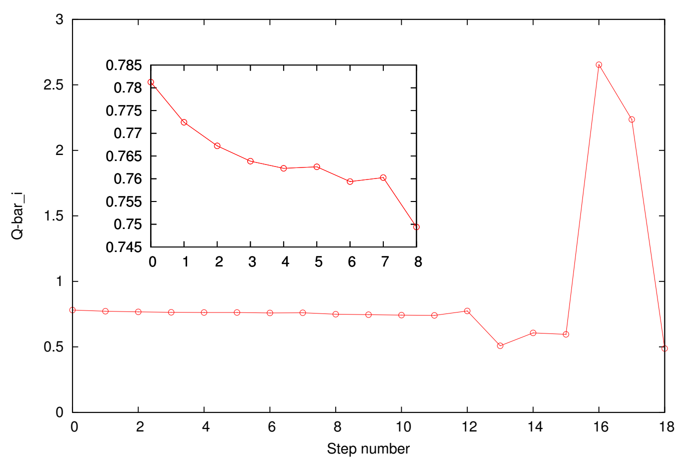

Fig. 4. Evolution of $\bar{Q}$ in semi-passive dynamic walking where $T_{\rm set} = 0.1$ [s], $u_0 = 1.0$ [N·m] and $\phi = 0.1$ [rad]

result indicated, the values of $\bar{Q}$ in all cases monotonically increase with the increase of $T_{\rm set}$. The numerically integrated values in the real walking systems are slightly larger than the analytical solution. This might be caused by the facts that the error terms in Eqs. (25) and(27) are non-negligible and that the initial error of 0.2 [rad/s] is too large.

B. *Effect of* u_0

Next, we analyze the effect of u_0. Fig. 6 plots $\bar{Q}$ of Eq. (51) in the linear and the nonlinear models and the analytical solution of $\bar{Q}$ of Eq. (47) with respect to u_0 where $M = 1.0$ [kg], $l = 1.0$ [m], $T_{\rm set} = 0.1$ [s] and $\phi = 0.1$ [rad]. As the mathematical result indicated, the values of $\bar{Q}$ in all cases monotonically increase with the increase of u_0. Acceleration worsens the convergence speed and deceleration improves it. As in the previous case, the numerically integrated values are slightly larger than the analytical solution. Nevertheless, the error is maintained at an acceptable level and analytical solution is useful for examining the convergence property without conducting numerical simulations.

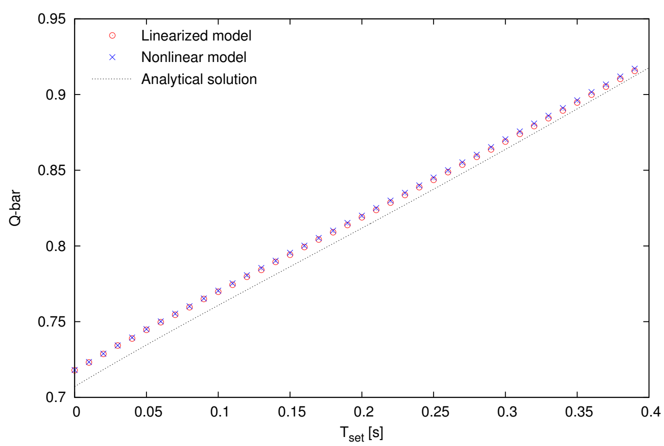

Fig. 5. $\bar{Q}$ in linearized and nonlinear model and its analytical solution with respect to $T_{\rm set}$ where $M = 1.0$ [kg], $l = 1.0$ [m], $u_0 = 1.0$ [N·m] and $\phi = 0.1$ [rad]

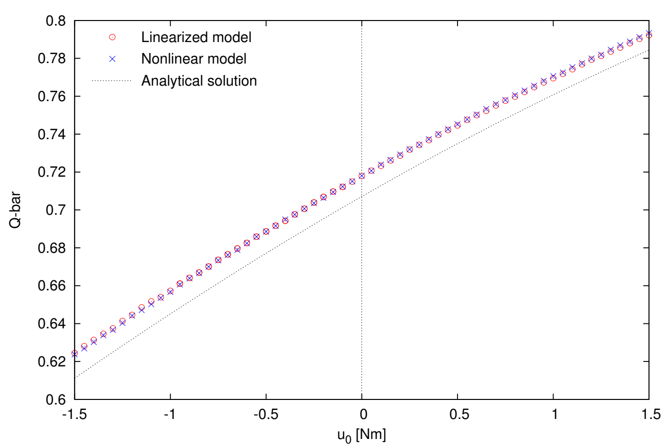

Fig. 6. $\bar{Q}$ in linearized and nonlinear model and its analytical solution with respect to u_0 where $M = 1.0$ [kg], $l = 1.0$ [m], $T_{\rm set} = 0.1$ [s] and $\phi = 0.1$ [rad]

VI. CONCLUSION AND FUTURE WORK

In this paper, we derived the analytical solution to the transition function of the state error for the stance phase in 1-DOF semi-passive dynamic walking. The numerical results in Section V suggested that the values of $\bar{Q}$ obtained numerically in the linearized and the nonlinear models are almost the same but they are slightly larger than the analytical solution. This implies that the error terms higher than second-order neglected in Eqs. (25) and (27) are not sufficiently small and that the analytical solution is valid only for sufficiently-small state errors.

In the future, we should analyze the effective range of the analytical solution and consider the methods for improving the accuracy of the analytical solution. The control parameters, u_0 and $T_{\rm set}$, that achieve the deadbeat mode, $\bar{Q} = 0$, can be uniquely determined by Eq. (47) and the parameters for deadbeat gait generation are then obtained by solving the equation. Development of some useful solutions for it is left as a future work.

The method in this paper can be applied to other walking systems where the state transition during the stance phases can be described in the same form as Eq. (18). Now we are analyzing the stability of an underactuated bipedal gait with constraint on impact posture [7]. The result will be reported in a future paper.

ACKNOWLEDGMENT

This research was partially supported by a Grant-in-Aid for Scientific Research, (C) No. 24560542, provided by the Japan Society for the Promotion of Science (JSPS).

REFERENCES

[1] T. McGeer, "Passive dynamic walking," *Int. J. of Robotics Research*, Vol. 9, No. 2, pp. 62–82, 1990.
[2] A. Goswami, B. Thuilot and B. Espiau, "A study of the passive gait of a compass-like biped robot: symmetry and chaos," *Int. J. of Robotics Research*, Vol. 17, No. 12, pp. 1282–1301, 1998.
[3] J. W. Grizzle, G. Abba and F. Plestan, "Asymptotically stable walking for biped robots: Analysis via systems with impulse effects," *IEEE Trans. on Automatic Control*, Vol. 46, No. 1, pp. 51–64, 2001.
[4] D. G. E. Hobbelen and M. Wisse, "A disturbance rejection measure for limit cycle walkers: The gait sensitivity norm," *IEEE Trans. on Robotics*, Vol. 23, No. 6, pp. 1213–1224, 2007.
[5] F. Asano, "Stability analysis of passive compass gait using linearized model," *Proc. of the IEEE Int. Conf. on Robotics and Automation*, pp. 557–562, 2011.
[6] F. Asano, "Stability principle underlying passive dynamic walking of rimless wheel," *Proc. of the IEEE Int. Conf. on Control Applications*, pp. 1039–1044, 2012.
[7] F. Asano, "Stability analysis of underactuated bipedal gait using linearized model," *Proc. of the 11th IEEE-RAS Int. Conf. on Humanoid Robots*, pp. 282–287, 2011.
[8] F. Asano, "Fast convergent gait generation of underactuated biped based on output deadbeat control," *Proc. of the 12th IEEE-RAS Int. Conf. on Humanoid Robots*, pp. 90–95, 2012.
[9] M. J. Coleman, A. Chatterjee and A. Ruina, "Motions of a rimless spoked wheel: a simple three-dimensional system with impacts," *Dynamics and Stability of Systems*, Vol. 12, Iss. 3, pp. 139–159, 1997.
[10] F. Asano and X. Xiao, "Output deadbeat control approaches to fast convergent gait generation of underactuated spoked walker," *Proc. of the IEEE/SICE Int. Symp. on System Integration (SII)*, pp. 265–270, 2012.
[11] F. Asano and X. Xiao, "Role of deceleration effect in efficient and fast convergent gait generation," *Proc. of the IEEE Int. Conf. on Robotics and Automation*, pp. 5649–5654, 2013.